THE FUNDAMENTAL SHOCK-VORTEX INTERACTION PATTERNS THAT DEPEND ON THE VORTEX FLOW REGIMES

Keun-Shik Chang,[*1] Hrushikesh Barik[1] and Se-Myong Chang[2]

The shock wave is deformed and the vortex is elongated simultaneously during the shock-vortex interaction. More precisely, the shock wave is deformed to a S-shape, consisting of a leading shock and a lagging shock by which the corresponding local vortex flows are accelerated and decelerated, respectively: the vortex flow swept by the leading shock is locally expanded and the one behind the lagging shock is locally compressed. As the leading shock escapes the vortex in the order of microseconds, the expanded flow region is quickly changed to a compression region due to the implosion effect. An induced shock is developed here and propagated against the vortex flow. This happens for a strong vortex because the tangential flow velocity of the vortex core is high enough to make the induced-shock wave speed supersonic relative to the vortex flow. For a weak shock, the vortex is basically subsonic and the induced shock wave is absent. For a vortex of intermediate strength, an induced shock wave is developed in the supersonic region but dissipated prematurely in the subsonic region. We have expounded these three shock-vortex interaction patterns that depend on the vortex flow regime using a third-order ENO method and numerical shadowgraphs.

Key Words : Shock-vortex interaction, Transonic vortex, Induced shock wave, Composite vortex model, Implosion effect

1. INTRODUCTION

Shock-vortex interaction is important to understand the basic noise generation mechanisms of the high speed flow. Noise sources such as the screech tones and the crackles, for example, are produced in the jet when shocks interact with the turbulent eddies[1]. Depending on strengths of the interacting shock wave and the vortex, the patterns of shock-vortex interaction appear quite diverse. Earlier investigations have emphasized on the nature of acoustic noise generation due to shock-vortex interactions[2,3]. The detailed shock-vortex interaction patterns are closely related to the noise generation mechanisms and worthy of investigation. Later studies have studied the different shock-vortex interaction patterns brought about by diverse interactions among the incident shock, the secondary shock, the primary vortex and the secondary vortexlets[4-7].

Earlier study was based on the linear theory, assuming small deflection of the incident shock wave. Ribner[3] explained how the radial acoustic waves were related to the quadrupolar noise sources. Nonlinear deformation of the shock was investigated numerically[5-10]. In particular, Ellzey et al.[4] have indicated that the captured shock interacts with the accelerated shock to create quadrupolar acoustic noise sources. Chatterjee[10] indicated that shock-shock interaction changed from MR type to RR type as the incident shock Mach number was decreased while the vortex was maintained at a constant strength. In this paper we elaborate that the shock-vortex interaction patterns can be significantly different depending on the vortex flow regime.

First of all we investigate the physics of shock-vortex interaction. When the interacting shock and the vortex are both strong, deformation of the S-shape shock and elongation of the elliptic vortex are both severe. As the

Received: June 30, 2009, Revised: August 17, 2009, Accepted: August 21, 2009.

1 Department of Mechanical and Aerospace Engineering Systems, KAIST, Daejeon 305-701, Republic of Korea

2 School of Mechanical Engineering, Kunsan National University, Kunsan-shi, Jollabuk-do 573-701 Republic of Korea

* Corresponding author, E-mail: kschang@kaist.ac.kr

incident shock is advanced to the vortex, in fact, one part is accelerated by the favorable vortex direction to become a leading shock and another part is decelerated by the adverse vortex direction, becoming a lagging shock. A low-pressure expansion region is created in a vertex of the elongated vortex or in the region swept by the leading shock. It is in contrast to the high-pressure compression region created in the other vertex of the elongated vortex that is in the region swept by the lagging shock. A dipole pressure distribution is created as a result in the elongated vortex. The expansion region is first small but grows in time, as the shock is advanced in the vortex.

When the shock departs the vortex core, the departure time is very short and it is in the order of micro seconds. Departure of the shock is not made instantly either: the leading shock escapes the vortex first and the lagging shock is held by the vortex quite long. When the leading shock has departed the vortex, the expansion region is changed quickly to a compression region in the elongated tip of the vortex because of the implosion effect. This compression region would spread in time with two frontal waves moving in opposite directions: an induced expansion wave moves in the vortex direction and an induced shock wave moves against the vortex direction. A second dipole pressure structure is created as a consequence, making the overall pressure a quadrupolar structure.

Outside the vortex core, the leading shock has escaped the vortex to become the so-called 'accelerated shock'. It is in contrast to the lagging shock that is held by the vortex core: we call it simply a ‘captured shock’. The two shocks make first a RR (Regular Reflection) in the shock-shock interaction but later become MR (Mach Reflection) with the structure of a Mach stem, two triple points and two slip lines that spiral into the vortex core.

In this paper, we identify three different shock-vortex interaction patterns. One is the Interaction Type I, created by a weak shock-vortex interaction or by a weak vortex that has basically subsonic velocities everywhere in the vortex core. It shows no evidence that the afore-mentioned induced shock has ever developed. The other is the Interaction Type II, caused by a strong shock-vortex interaction or by a strong vortex that has a significant area of supersonic tangential velocity in the vortex core. The third is the Interaction Type III, that is caused by a shock-vortex interaction of moderate strength or by a transonic vortex that has a minimal supersonic area in an otherwise subsonic vortex core. Here an induced shock is developed in the supersonic area but dissipated prematurely into an acoustic wave in the subsonic area. We will indicate that this Interaction Type III takes a very narrow band in the parameter plane, suggesting a critical area separating the more stable Interaction Type I and Type II.

2. GOVERNING EQUATIONS, NUMERICAL SCHEME AND INITIAL CONDITIONS

We employ a third-order Essentially Non-Oscillatory (ENO) scheme[11,12] to solve the unsteady two-dimensional Euler equations. It is well known that ENO schemes can resolve aeroacoustic pressure fields comprising both shocks and acoustic waves. We take the two-dimensional unsteady Euler equations in the conservative form.

We choose a composite vortex model similar to the one taken by Ellzey et al.[4]. It consists of an inner vortex core represented by

$$U_\theta(r) = \frac{U_c r}{R_c}, r < R_c \tag{1}$$

and an outer vortex flow given by

$$U_\theta(r) = Ar + \frac{B}{r}, R_c \le r \le R_o \tag{2}$$

where U_θ =tangential velocity, U_c =maximum tangential velocity, r =distance from the vortex center, R_c =vortex core radius, and R_o =outer radius. The coefficients A and B in the Equation (2) are chosen so that $U_\theta = U_o$ when $r = R_c$ and $U_\theta \to 0$ when $r = R_o$. Outside $r = R_o$, the velocity is taken zero everywhere. The initial pressure is specified such that the pressure gradient always balances the centripetal force as in

$$\frac{\partial p}{\partial r} = \rho \frac{U_\theta^2}{r} \tag{3}$$

In this work, a planar shock wave travels from right to left to interact with a compressible vortex rotating counterclockwise. The computational domain is 10cm X 10cm and It is covered by 960 x 960 uniform grid. The initial condition is prescribed by Rankine-Hugoniot relations on the shock wave and ambient conditions elsewhere. For all open boundaries, conventional characteristic boundary conditions are prescribed using the Riemann invariants[10].

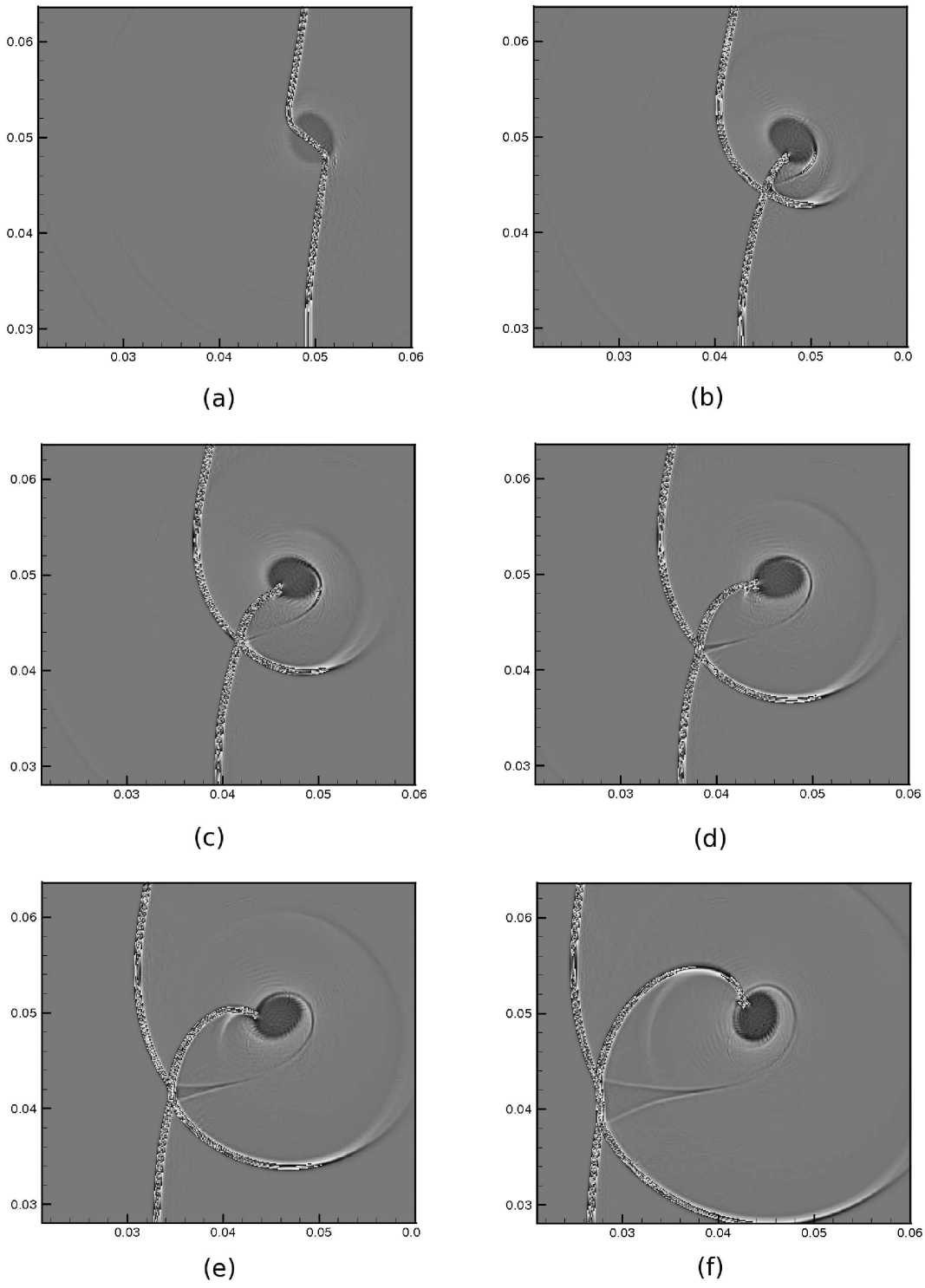

Fig. 1 Numerical shadowgraphs at different time instants: Type I interaction (Ms=1.2 & Mv=0.7)

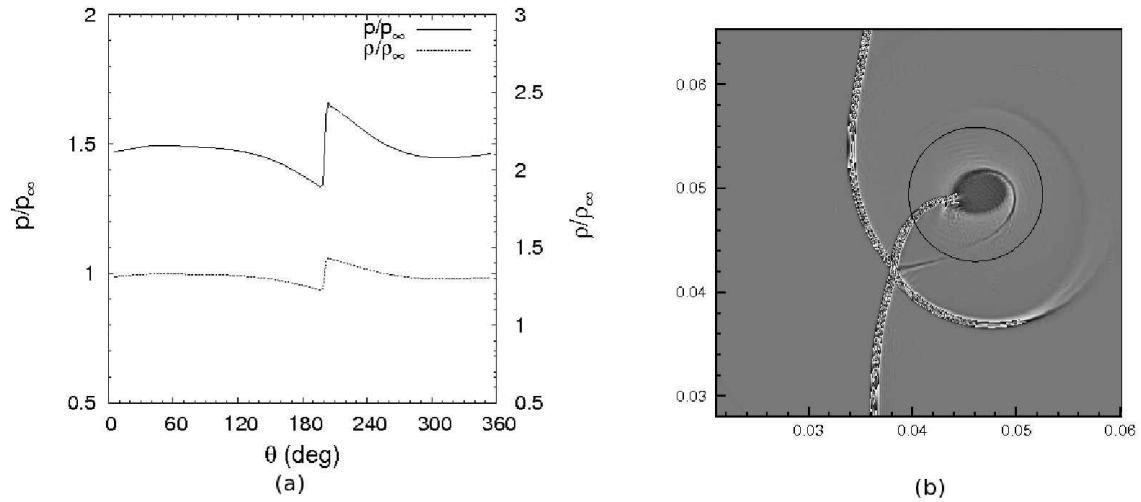

Fig. 2 (a) Circumferential pressure and density variation on a circle of radius 0.64 cm; (b) A circle shown in the vortex of Fig. 1(d)

The accuracy of present numerical results has been validated in a companion paper[13] by comparing the circumferential acoustic pressure with the experimental data[2] for the shock-vortex interaction made for Ms=1.29 and Mv=0.52. The grid dependency has been also examined: consistent results have been obtained for grid number higher than 480x480.

3. SHOCK-VORTEX INTERACTION PATTERNS

In the present work, 42 parametric cases of shock-vortex interaction have been tested. The upper bound of parameter is 1.6 for the shock Mach numbers(Ms) and 1.2 for the maximum vortex Mach numbers(Mv). This parameter range is broad enough to encompass most of the earlier shock-vortex interaction cases in the literature. We have obtained numerical shadowgraphs and circumferential pressure plus density variations to look at the detailed physics of the different Interaction Types.

3.1 INTERACTION TYPE I

In Fig. 1, the Interaction Type I is presented using a number of numerical shadowgraphs as the first gradient of the density. This case corresponds to a weak shock-vortex interaction for which the parameters are set to shock Mach number Ms=1.2 and subsonic maximum vortex Mach number, Mv=0.7. In Fig. 1(a), the incident shock is mildly deformed to a S-shape: the flow swept by the leading shock is accelerated but not enough to attain a supersonic speed. In Fig. 1(b), the flow behind the lagging shock or the captured shock is decelerated and compressed.

The accelerated shock partly encircling the disturbed vortex makes first a RR in the shock-shock interaction with the captured shock. A slip line is emanated from the triple point and landed on the vortex core that is gyrating anticlockwise. The interaction later becomes a MR with two triple points and two slip lines: see Fig. 1(e)-1(f). The captured shock moves clockwise against vortex direction and is reflected from the vortex core to produce a weak expansion wave. Opposite to the captured shock, no induced shock is observed in the outer vortex.

Fig. 2(a) shows distribution of the density and the pressure along a circle that is situated in the physical domain as shown in Fig. 2(b). It suggests that the anticlockwise vortex flow experiences a significant flow expansion that is terminated by a captured shock at Θ =210 (Θ=0 is in the east); also a smooth compression follows a smooth expansion.

3.3 INTERACTION TYPE II

Fig. 3 shows the numerical shadowgraphs obtained by a strong shock-vortex interaction for which Ms=1.6 and Mv=1.0. For these parameters, a substantial area of the vortex does attain supersonic speeds. In Fig. 3(a) the shock begins to deform and the vortex begins to elongate severely. In Fig. 3(b) the leading shock is observed about to depart the vortex, leaving an expansion region in its wake: the lagging shock is extended upward a little to be

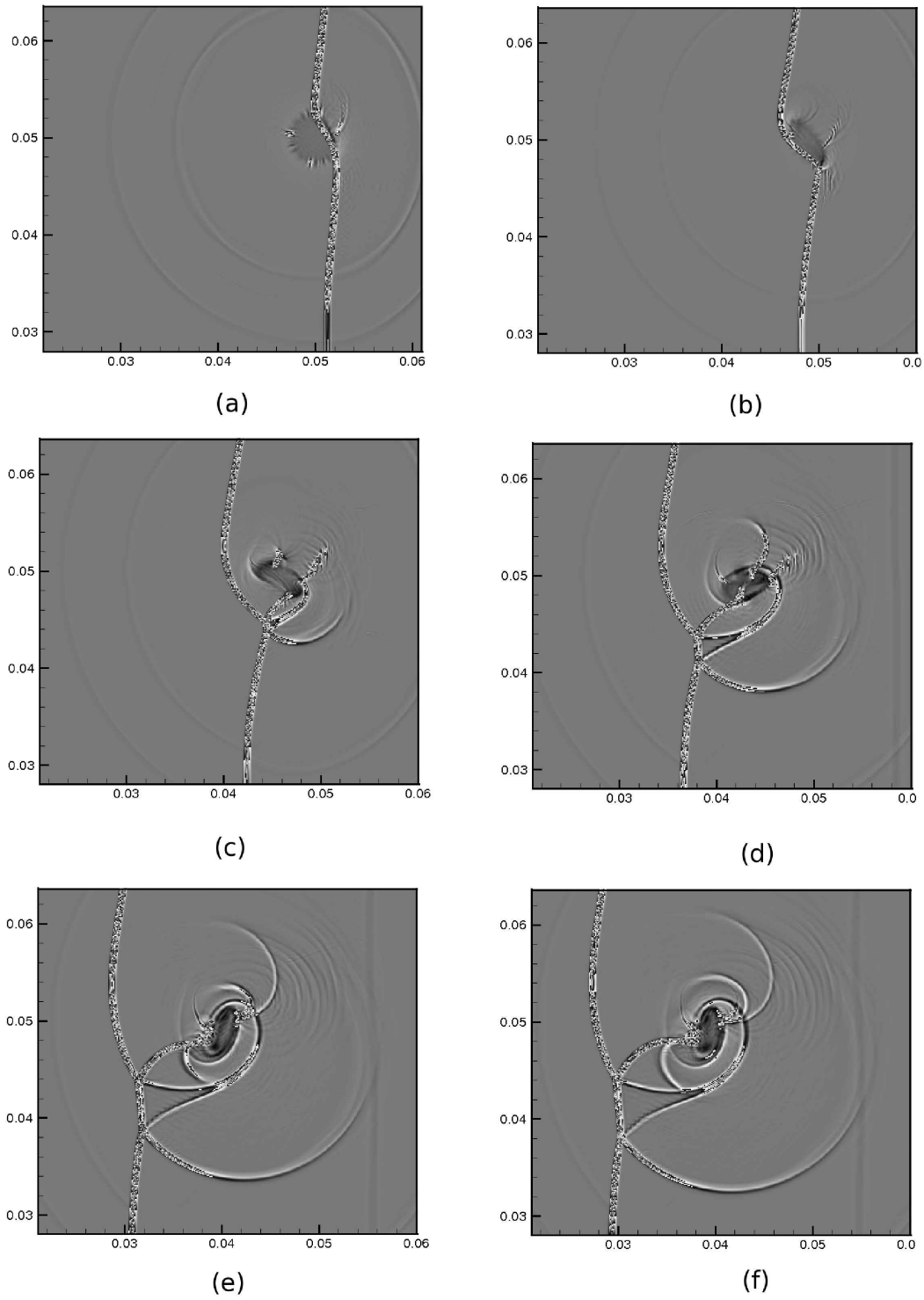

Fig. 3 Numerical shadowgraphs at different time instants: Type II interaction (Ms=1.6 & Mv=1.0)

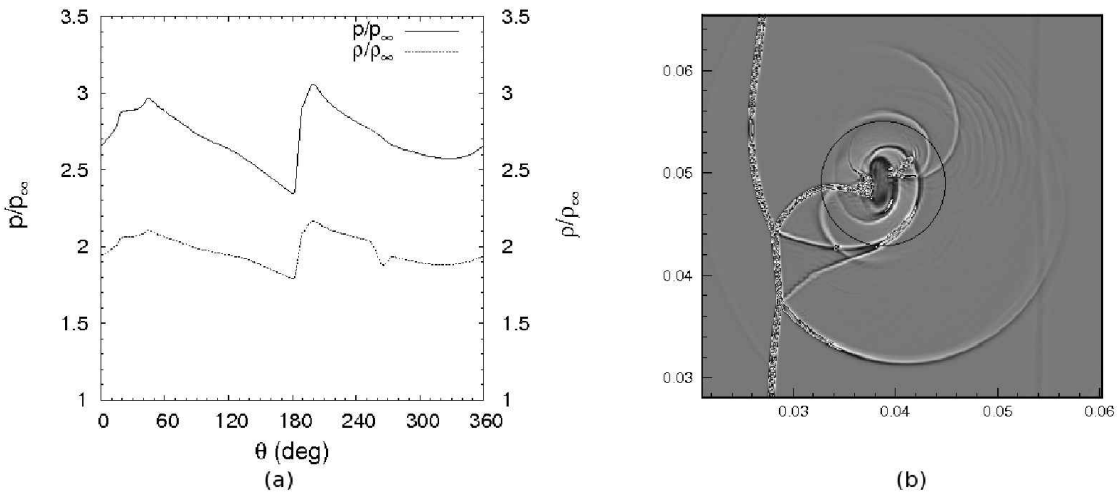

Fig. 4 (a) Circumferential pressure and density variation on a circle of radius 0.61 cm; (b) A circle shown in the vortex of Fig.3(d)

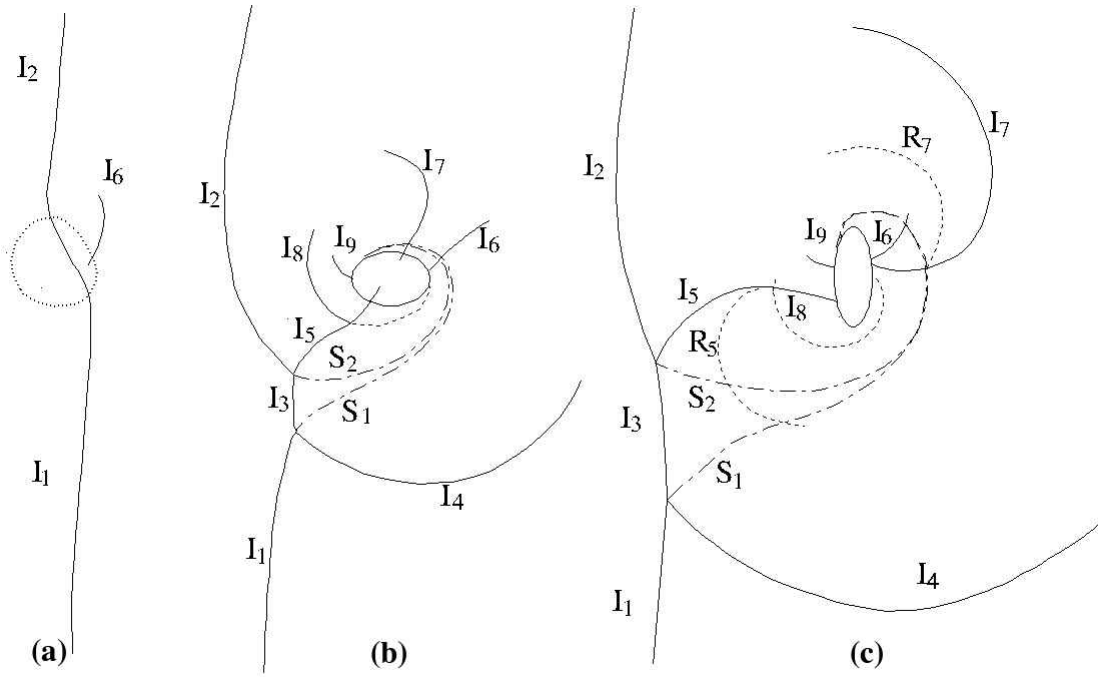

Fig. 5 Schematic diagrams: Type II interaction

a 'transmitted shock'.

After departure from the vortex the leading shock is changed to an accelerated shock moving away from the vortex. The expansion region is then quickly changed to a compression region due to the implosion effect. A high pressure begins to accumulate in the ex-expansion region in the upper elongated tip of the vortex. The new compression region spreads in time with two frontal waves: an induced expansion wave moving with the vortex flow and an induced shock wave moving against

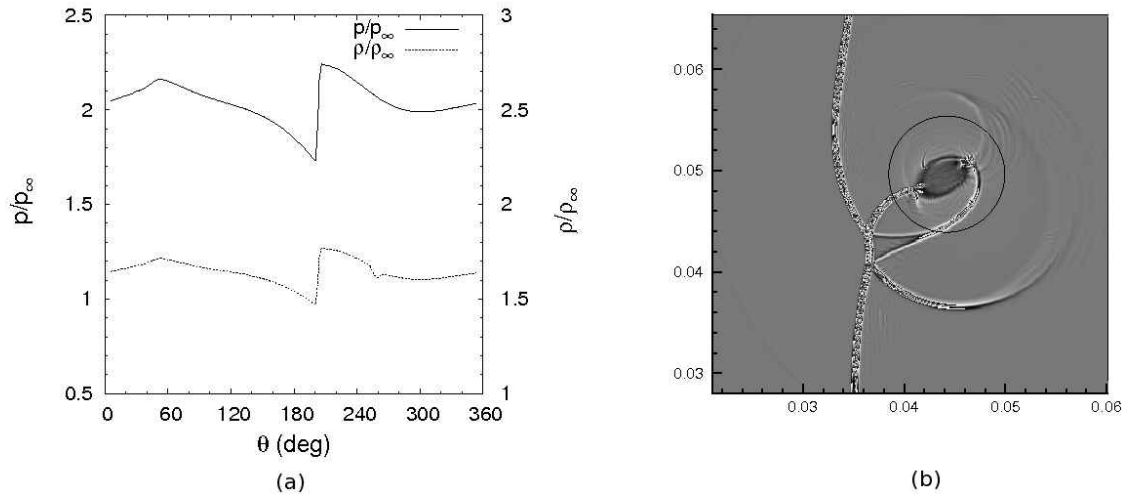

Fig. 7(a) Circumferential pressure and density variation on a circle of radius 0.57 cm; (b) A circle shown in the vortex of Fig. 6(d)

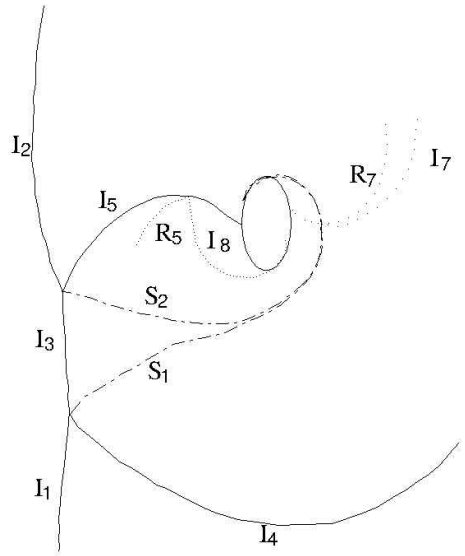

Fig. 8 A schematic diagram : Type III interaction

the vortex flow, see Fig. 3(c). These waves are observed grown up in Fig. 3(d).

In Fig. 3(e), a reflected expansion waves is created by reflection of the captured shock from the vortex core. Another reflected expansion wave is observed at the induced shock wave that is again reflected from the vortex core. Separate study has shown that the reflected wave is generated whenever a shock wave hits the elongated tip of the elliptic vortex. The induced expansion wave is rotated with the gyrating vortex and makes intersection with the captured shock as in Fig. 3(e) and 3(f), landing on the vortex core in a spiral form similar to the slip lines. In the Type II interaction, it is interesting to observe that the captured shock and the induced shock look alike. In Fig. 4(a), a quadrupolar pressure structure is indicated by the pressure and density distributions that are plotted along a circle shown in Fig. 4(b). In the density distribution curve shown in Fig. 4(a) and Fig 7(a), there is a small dip at about Θ=260 degrees because of the strong slip line. It is in contrast to Fig. 2(a) where the density curve does not show distinct slip line effect.

It is noted that the induced shock would never become fully developed unless the vortex flow has substantial supersonic area. In the Type I interaction, the vortex was subsonic everywhere. The vortex flow has therefore adjusted continuously in the circumferential direction to meet the flow conditions of the captured shock. In the Type III interaction, adjustment of the vortex flow is not so smooth as the Type I since disturbance signals cannot propagate upwind of a supersonic flow. An induced shock is instead developed to make the vortex flow slow down to a subsonic speed. The vortex flow hereby can adjust to the conditions of the captured shock after the induced shock. It is noted that even a small shocklet is necessary for minor adjustment as observed in Fig. 3(d)-3(f).

A schematic diagram in Fig. 5(a) shows that, when a shock advances in the vortex, the impinging shock is deformed to the leading shock I_2, a lagging shock I_1 and a transmitted shock I_6. In Fig. 5(b), the leading shock escaped the vortex and became an accelerated shock, I_2

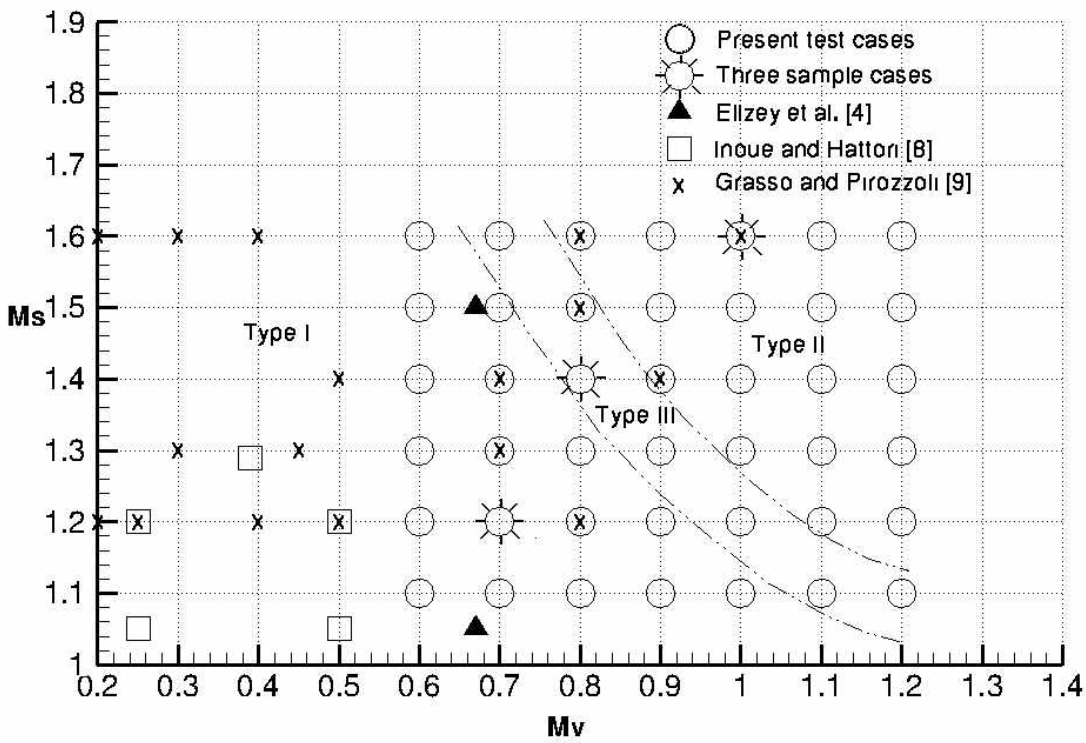

Fig. 9 A parameter map showing the three regions of interaction types

plus I_4. It makes a Mach reflection with the captured shock, I_1 plus I_5, with a Mach stem I_3 and two slip lines S_1 and S_2 produced as a consequence. The pair of I_7 and I_8 are the induced shock and the induced expansion wave, respectively. The reflected waves are shown in Fig. 5(c): the induced shock I_7 is reflected as R_7 and the captured shock I_5 is reflected as R_5. The induced expansion wave I_8, that is rotated with the gyrating vortex, makes an intersection with the captured shock and is landed on the vortex core in a spiral form similar to the slip line. A small shocklet I_9 helps the flow to adjust as the flow is expanded, passing through the induced shock wave, until the induced expansion wave is encountered.

3.2 INTERACTION TYPE III

In Fig. 6, a Type III interaction is presented with Ms=1.4 and Mv=0.8. Here the expansion by the leading shock and the compression by the lagging shock are not as strong as the Type II interaction. As the leading shock has escaped the vortex, we observe that there is a usual compression area developing in the upper elongated tip of the vortex. This area grows with the induced shock wave moving clockwise and the induced expansion wave moving anticlockwise similarly to the Type II. The induced shock is, however, dissipated prematurely to an acoustic wave because the supersonic area is limited in the vortex for this parameter case: see Fig. 6(e) and 6(f). In the circumferential pressure and density distributions shown in Fig. 7, we observe , at about Θ=50 degrees opposite to the captured shock at Θ=210 degree, that there is a compression wave, not an induced shock.

Fig. 8 shows a schematic diagram of the Type III interaction. The captured shock I_5 has developed a reflection wave R_5. The induced expansion wave I_8 makes intersection with I_5. Opposite to the captured shock I_5, we have suggested by two sparsely dashed lines that the induced shock wave I_7 and its reflected wave R_7 are dissipated prematurely into weak acoustic waves as they are further propagated.

4. PARAMETER MAP

Fig. 9 is a Ms-Mv parameter map from which we can observe where a certain type of shock-vortex interaction is

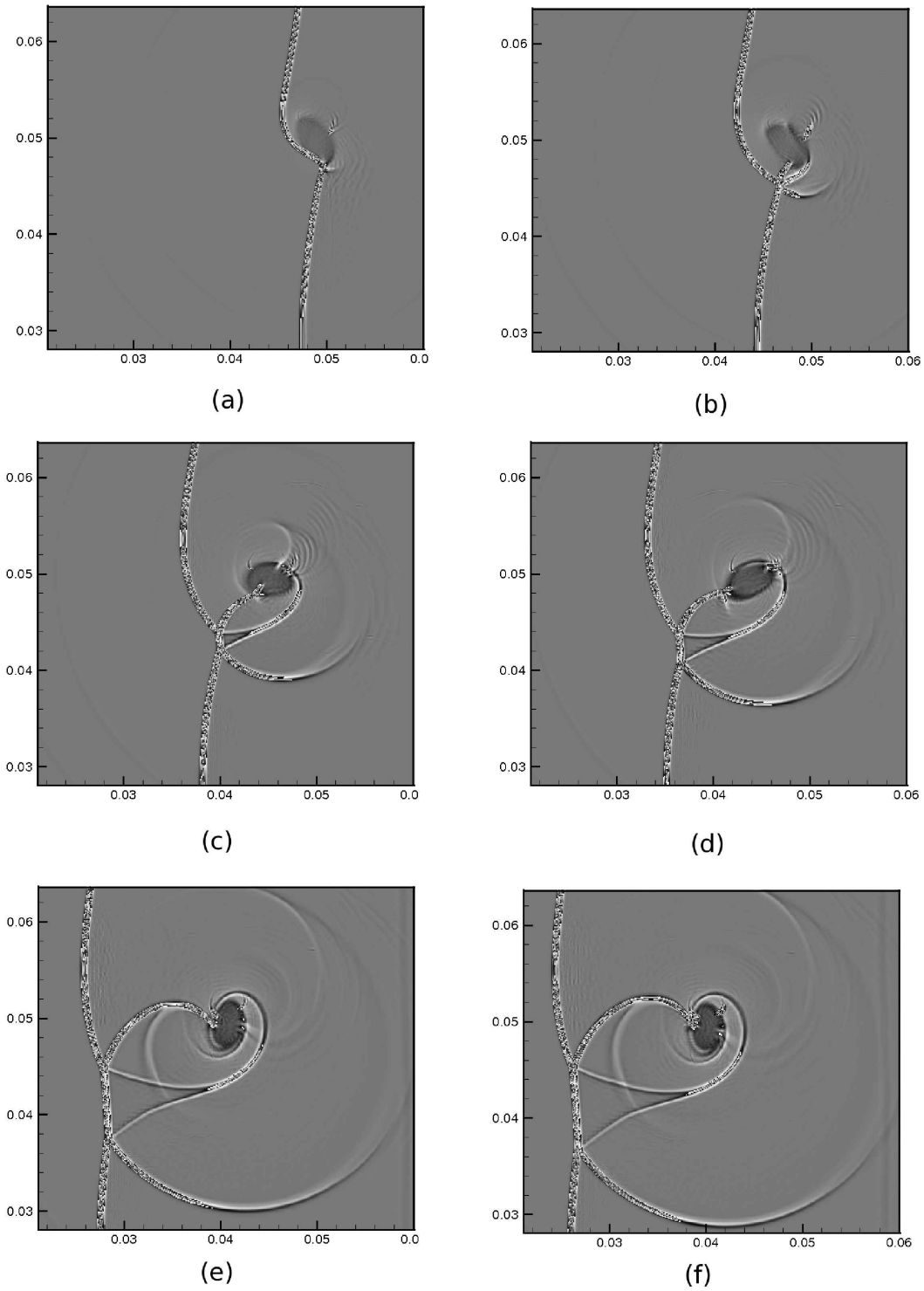

Fig. 6 Numerical shadowgraphs at different time instants: Type III interaction (Ms=1.4 & Mv=0.8)

located. We have tested 42 parametric cases as they are marked by empty circles. The three sample cases presented in this paper by shadowgraphs are marked by solar symbols. Other symbols indicate those parametric cases that have been investigated by other researchers. We have determined what type of interaction a particular parameter set will actually have by inspecting the numerical shadowgraphs and circumferential pressure curves. It is noted that the Type III region takes a very narrow, banded region in the parameter map. It can be considered, therefore, the parameter set for the Type III interaction is a critical one that separates the more stable Type I and Type II interactions.

5. CONCLUSIONS

Shock-vortex interaction patterns have been expounded by identifying three different interaction types that depend on the vortex flow regime. We have discussed how these interaction types are different from one another and why particular types should take place physically. A conclusion can be made that the most distinguished feature of the shock-vortex interaction is onset of the induced expansion and induced shock waves for the strong interactions. For the weak interactions, the induced shock wave does not develop. For the critical intermediate parameter set, the induced shock wave is developed but prematurely dissipated due to the transonic nature of the vortex flow. These interaction patterns should have a close relation with a certain type of noises generated by shock-vortex interactions in the high speed jets.

ACKNOWLEDGEMENT

The research has been financially aided by Brain Korea 21 program(KAIST Valuefacture Institute of Mechanical Engineering), sponsored by Ministry of Education, Science and Technology, Republic of Korea.

REFERENCES

[1] 1997, Ffowcs, W.J.E., Simson, J. and Vichis, V.J., "'Crackle': an annoying component of jet noise," *Journal of Fluid Mechanics*, Vol.7, pp.251-271.

[2] 1965, Dosanjh, D.S. and Weeks, T.M., "Interaction of a starting vortex as well as a vortex street with a traveling shock wave," *AIAA Journal*, Vol.3, pp.216-223.

[3] 1985, Ribner, H.S., "Cylindrical sound wave generated by shock vortex interaction," *AIAA Journal*, Vol.23, pp.1708-1715.

[4] 1995, Ellzey, J.L., Henneke, M.R., Picone, J.M. and Oran, E.S., "The interaction of a shock with a vortex: Shock distortion and the production of acoustic waves," *Phys. of Fluid*, Vol.7, pp.172-183.

[5] 2000, Chang, S.-M. and Chang, K.-S., "Visualization of Shock-Vortex Interaction Radiating Acoustic Waves," *Journal of Visualization*, Vol.3, pp.221-228.

[6] 2004, Chang, K.-S. and Chang, S.-M., "Scattering of Acoustic waves in Shock-Vortex Interaction," *Materials Science Forum*, Vol.465-466, pp.131-138.

[7] 2004, Chang, S.-M., Chang, K.-S. and Lee, S., "Reflection and Penetration of Shock Wave Interacting with a Starting Vortex," *AIAA Journal*, Vol.42(4), pp.796-805.

[8] 1999, Inoue, O. and Hattori, Y., "Sound generation by shock-vortex interactions," *Journal of Fluid Mechanics*, Vol.380, pp.81-116.

[9] 2000, Grasso, F. and Pirozzoli, S., "Shock-wave-vortex interactions: Shock and vortex deformations and sound production," *Theoretical and Computational Fluid Dynamics*, Vol.13, pp.421-456.

[10] 1999, Chatterjee, A., "Shock waves deformation in shock-vortex interactions," *Shock Waves*, Vol.9, pp.95-105.

[11] 1988, Shu, C.W. and Osher, S., "Efficient implementation of essentially non-oscillatory shock-capturing schemes," *Journal of Computational Physics*, Vol.77, pp.439-471.

[12] 1989, Shu, C.W. and Osher, S., "Efficient implementation of essentially non-oscillatory shock-capturing schemes, ii," *Journal of Computational Physics*, Vol.83, pp.32-78.

[13] 2009, Chang, K.-S., Barik, H. and Chang, S.-M., "The shock-vortx interaction patterns affected by vortex flow regime and vortex models," *Shock Waves*, Vol.19, pp.349-360.